

---

# The Location of Transition States: A Comparison of Cartesian, Z-Matrix, and Natural Internal Coordinates

---

JON BAKER\* and FORA CHAN

*BIOSYM Technologies, Inc., 9685 Scranton Road, San Diego, California 92121-3752*

*Received 21 March 1995; accepted 5 July 1995*

---

## ABSTRACT

A comparison is made between geometry optimization in Cartesian coordinates, in Z-matrix coordinates, and in natural internal coordinates for the location of transition states. In contrast to the situation with minima, where all three coordinate systems are of comparable efficiency if a reliable estimate of the Hessian matrix is available at the starting geometry, results for 25 different transition states covering a wide range of structural types demonstrate that in practice Z-matrix coordinates are generally superior. For Cartesian coordinates, the commonly used Hessian update schemes are unable to guarantee preservation of the necessary transition state eigenvalue structure, while current algorithms for generating natural internal coordinates may have difficulty handling the distorted geometries associated with transition states. The widely used Eigenvector Following (EF) algorithm is shown to be extremely efficient for optimizing transition states. © 1996 by John Wiley & Sons, Inc.

---

## Introduction

There has been increasing interest in recent years in geometry optimization directly in Cartesian coordinates as opposed to the perhaps more traditional—certainly among quantum chemists—use of internal coordinates. The latter are usually implemented via the well-known Z-

matrix formalism, with the Z-matrix serving both as a definition of the coordinate system and a means of inputting the molecular geometry.

The principal factor in the renewed use of Cartesian coordinates has been the—now widespread—availability of graphical model builders, which are being utilized to construct not just large molecules, such as proteins necessary in drug design, but also smaller systems more amenable to investigation using quantum mechanics. Because the final geometry resulting from the model-building process—often involving a preliminary optimization using a molecular mechanics force field

\*Author to whom all correspondence should be addressed at Department of Chemistry, University of Arkansas, Fayetteville, Arkansas 72702.

—is a set of Cartesian coordinates, it is clearly advantageous if the higher-level (quantum) optimization be done directly in Cartesians. It is now well established that *minimization* in Cartesian and Z-matrix coordinates is of comparable efficiency provided a reliable estimate of the Hessian (second derivative) matrix is available at the (reasonable) starting geometry.<sup>1</sup> A simple mechanics Hessian is usually perfectly adequate for this purpose.

An alternative to both Cartesian and Z-matrix coordinates are the so-called natural internal coordinates, proposed in this context by Pulay.<sup>2,3</sup> These involve linear combinations of bond angles and torsions as deformational coordinates constructed (using approximate local symmetry around certain atomic centers or in certain regions of the molecular system, e.g., rings) in such a way so as to minimize the coupling between the various coordinates. One clear advantage internal coordinates have always possessed over Cartesians is that a well-chosen set of internals is much more decoupled than the corresponding Cartesian coordinates, and natural internal coordinates exploit this advantage to the full, providing coordinates that are essentially decoupled to the maximum extent possible. What this means in practice is that optimizations in natural internals are much less sensitive to the quality of the starting Hessian than are Cartesian optimizations and are especially insensitive to off-diagonal (coupling) Hessian matrix elements. Furthermore, natural internal coordinates can be generated directly from Cartesian coordinates themselves, and so—although they are somewhat complicated—no user input is required to define them. However, it has again been demonstrated (exactly analogous to Z-matrix coordinates) that, with a reliable starting Hessian, minimization in Cartesian and natural internal coordinates is also of comparable efficiency.<sup>4</sup> Additionally, there are certain advantages in using Cartesian coordinates when searching for local (metastable) minima.<sup>4</sup>

Transition states are typically far more difficult to locate than minima due almost entirely to their much greater sensitivity to the Hessian eigenvalue structure; this is true regardless of the coordinate system used to carry out the optimization (Cartesians or internals). At a stationary point corresponding to a transition state, the Hessian matrix must have one and only one negative eigenvalue; furthermore, it must be the right negative eigenvalue (i.e., the corresponding eigenmode must be such that deformation of the molecular structure along this direction on the potential energy surface

connects the transition state to the reactants and products of interest).

Location of transition states is also hindered by the fact that, unlike minima, there are no generally available force fields suitable for determining transition state geometries or, indeed, model builders capable of building suitable starting structures with the same ease as for normal, stable molecules. In many cases an initial geometry is constructed using chemical intuition, and the search proceeds from there. This inevitably means that starting geometries for transition state searches are typically much worse (i.e., farther from the final converged structure) than are those for minimization. A commonly employed tactic is to select a suitable (internal) coordinate as the reaction coordinate and do a limited potential scan along this coordinate, with a full minimization in the space of the remaining variables at each point. The highest energy point along this "reaction path" is then taken as the starting guess for the transition state. No matter what method is used to derive an initial guess for the transition state geometry, a reliable Hessian must be provided, at least as far as the active site is concerned.

For natural internal coordinate optimizations, the geometrical distortions from standard structures associated with transition states are a potential source of problems. Natural internals were designed to exploit local symmetry (e.g., the bond angle around a formally  $sp^3$  hybridized carbon center is approximately tetrahedral regardless of the functional groups attached), and the fact that this no longer holds around the active site in a transition state could cause algorithms designed for optimizing minima to generate an inappropriate or unsuitable set of natural internal coordinates for optimizing transition states. Additional atom connectivity data may also be needed (e.g., for a dissociation reaction) in order to generate a full set of coordinates in cases where distances between atoms are so long as to preclude the assignment of a formal bond.

Given a starting geometry and a suitable Hessian, this article presents a comparison between optimizations carried out in Cartesian, Z-matrix, and natural internal coordinates, contrasting their relative efficiencies in locating the final optimized transition state geometry for a test suite of 25 reactions. In this regard, this work is a follow-up to a previous article published in this journal<sup>4</sup> which presented a similar comparison between Cartesians and natural internals for minimization. As in the previous study,<sup>4</sup> all starting geometries

(as Z-matrices) and initial and final energies are reported along with the number of cycles required to reach convergence. The test suite encompasses a wide range of reactions and transition structures and, it is hoped, will provide a standard by which to judge the usefulness of future developments in algorithms for locating transition states.

---

## Methodology

All optimizations, for all coordinate systems, were carried out using the Eigenvector Following (EF) algorithm<sup>5</sup> at the Hartree-Fock (HF) level (restricted for closed-shell systems, unrestricted for open-shell) with the 3-21G basis set. The EF algorithm, based on the work of Cerjan and Miller<sup>6</sup> and Simons and co-workers,<sup>7</sup> has been implemented in virtually all of the major computational quantum packages and is widely used to locate both transition states and minima.

Calculations were performed using the general-purpose optimization package OPTIMIZE<sup>8</sup> in conjunction with TURBOMOLE.<sup>9</sup> Natural internal coordinates were generated automatically from starting Cartesians using the algorithm built into OPTIMIZE (see ref. 4 for more details). Although they have been well tested for minima, natural internals are not commonly used for transition state optimizations and—as noted in the Introduction—the geometrical distortions from standard bond lengths and angles encountered in transition states could cause problems, both in generating and maintaining a suitable coordinate set. This will be particularly apparent for dissociation reactions, in which one molecule forms two (or more) fragments, with subsequent bond breaking and loss of formal bond connectivity. Consequently, for some of the systems studied, partial or forming/breaking bonds were formally taken to be full bonds and were added to the atom connectivity list; this was done so that OPTIMIZE could successfully generate a full set of natural internal coordinates. (Without such additional connectivity data, natural internals would be generated based on standard bond lengths and there would be an insufficient number of formal bonds to generate a full set of internals.)

Of the reactions in the test suite, several were taken from work done as part of a general validation of density functional methods<sup>10</sup>; there are three commonly used standards (the hydrogen cyanide/isocyanide and acetylene/ethynylidene

rearrangements and the dissociation of formaldehyde), and the remainder were culled from the (mainly recent) literature.

Four reactions in particular—rearrangement of the methoxy radical, ring opening of the cyclopropyl radical, ring opening of bicyclo[1.1.0]butane, and 1,2-migration in the  $\beta$ -(formyloxy) ethyl radical—were taken from a recent publication by Bofill.<sup>11</sup> In ref. 11, Bofill uses a restricted step algorithm to locate transition states and compares the efficiency of this method with that of the EF algorithm as implemented in the MOPAC<sup>12</sup> and GAMESS<sup>13</sup> programs. He also proposes an alternative Hessian update scheme—a linear combination of the well-known Powell<sup>14</sup> and Murtagh-Sargent<sup>15</sup> update formulas—which is claimed generally to perform better than either of the two standard updates separately.

Two of the four reactions taken from ref. 11 were studied by Bofill at the UHF/3-21G level, and we have used Bofill's starting geometries in order to make a direct comparison with his work. We also investigate Bofill's hybrid Hessian update scheme, comparing its performance with that of the Powell and Murtagh-Sargent updates alone.

---

## Results and Discussion

The reactions in the test suite cover a range of different types, including transition states for dissociation, insertion, rearrangement (e.g., hydrogen shifts), ring opening, and rotation. Most have low or no symmetry.

For each reaction transition state optimizations were carried out in Z-matrix, natural internal, and Cartesian coordinates. Within each coordinate set, four optimizations were performed on each system, each of which varied in the method used to update the Hessian (second derivative) matrix: (1) An exact Hessian matrix was calculated at each cycle (no updates were applied); (2) the Hessian matrix was updated using the Powell update<sup>14</sup>; (3) the Hessian was updated using the Murtagh-Sargent (MS) update<sup>15</sup>; and (4) the Hessian was updated using the hybrid Powell-MS scheme proposed by Bofill.<sup>11</sup> In every case an exact Hessian was always calculated at the starting geometry (cycle 1). A total of 12 transition state optimizations were thus undertaken for each of the 25 reactions in the test suite.

For each system, the Z-matrix optimizations were done first. In several cases starting geome-

known transition structures to prevent too rapid convergence and hence little or no difference in optimization performance between the various coordinate systems. Starting Cartesian coordinates were generated directly from the Z-matrices (with appropriate reorientation of axes where necessary to exploit molecular symmetry), and natural internal coordinates were in turn generated directly from the resultant Cartesians. As mentioned in the previous section, additional connectivity data was supplied in several cases in order to generate a full set of natural internals. Starting Z-matrices, initial energy, and final energy (at convergence) for each transition state are given in the Appendix.

Convergence criteria were the standard defaults of 0.0003 au on the maximum gradient component (Cartesian or internal where appropriate) and either an energy change from the previous cycle of less than  $10^{-6}$  hartree or a maximum predicted displacement of less than 0.0003 au per coordinate.

Optimizations in internal coordinates—both Z-matrix and natural internals—involve transformations of gradients and Hessian matrices from Cartesian coordinates—in which they are initially calculated—to the appropriate internal coordinate set. Such transformations require construction of the Wilson B-matrix.<sup>16</sup> Transformation of the Hessian matrix to internal coordinates included the gradient term derived from the derivative of the B-matrix. Inclusion of this term could change the eigenvalue structure of the transformed Hessian; in particular, initial starting Hessians in different coordinate systems—although derived from the same original Cartesian Hessian—need not possess the same number of negative eigenvalues.<sup>17</sup>

The reactions investigated in this work together with notes and references are shown in Table I. Optimization results (i.e., number of cycles to reach convergence) are given in Table II. Table III gives the number of negative eigenvalues in the starting Hessian within each coordinate system. This shows whether or not the optimization was started in a region of the potential energy surface with the right local curvature (transition states have one and only one negative eigenvalue in the Hessian matrix).

We turn first to the results with an exact Hessian matrix calculated at every cycle. These results provide an excellent standard since—with an exact Hessian—we are directly comparing the coordinate system uninfluenced by weaknesses or idiosyncracies in the various Hessian updating schemes; additionally, the number of cycles re-

quired to reach convergence is essentially a “best-case” scenario which can be used to judge the performance of the algorithm/updating scheme in the other cases.

Looking at the Z-matrix results (Table II), we see that all optimizations converged in eight cycles or less and typically around five cycles. This was the case even for the five systems with an initially incorrect Hessian eigenvalue structure (Table III). Furthermore, once the optimization algorithm had moved the system into a region of the potential energy surface (PES) with the required one negative eigenvalue, it never left it (i.e., once the correct Hessian eigenstructure was achieved, it was maintained to convergence). (This was also a feature of exact Hessian optimizations in Cartesian and natural internal coordinates as well.)

The natural internal coordinate results are generally very similar to the Z-matrix ones; however, there were a couple of systems (13 and 15, Table II) for which the natural internal optimization required three more cycles to converge than the corresponding Z-matrix optimization and three systems (6, 16, and 24) where the optimization failed.

Natural internal coordinate optimizations can fail in essentially three ways (other than simply failing to locate a stationary point in the maximum allowed number of cycles), all of which have to do with the coordinates themselves:

1. The assigning algorithm used to generate the natural internals from the input Cartesians is unable to generate a full set of linearly independent coordinates due, for example, to a complicated or undetermined molecular topology.
2. During the optimization a bond or dihedral angle becomes ill defined and there are problems forming the B-matrix.
3. The iterative procedure for transforming back from natural internal to Cartesian coordinates fails to converge and a new set of Cartesian coordinates is unavailable for the next cycle.

The first of these—the inability to generate a complete coordinate set—can be regarded as a weakness of the assigning algorithm which could potentially be eliminated by adding more options to the code, but even if coordinates could be generated in every possible situation, one would still have problems 2 and, especially, 3 to deal with. The

**TABLE I.**  
**Sources and References for the 25 Reactions Investigated.**

Reaction Investigated	Sources and References
1. $\text{HCN} \leftrightarrow \text{HNC}$	Starting geometry from Baker <sup>5</sup>
2. $\text{HCCH} \leftrightarrow \text{CCH}_2$	Starting geometry from Baker <sup>5</sup>
3. $\text{H}_2\text{CO} \leftrightarrow \text{H}_2 + \text{CO}$	
4. $\text{CH}_3\text{O} \leftrightarrow \text{CH}_2\text{OH}$	Starting geometry from Bofill <sup>11</sup>
5. ring opening cyclopropyl	Starting geometry from Bofill <sup>11</sup>
6. ring opening bicyclo[1.1.0] butane TS 1	Starting geometry from Bofill <sup>11</sup>
7. ring opening bicyclo[1.1.0] butane TS 2	Starting geometry from Bofill <sup>11</sup>
8. 1,2-migration -(formyloxy) ethyl	Starting geometry from Bofill <sup>11</sup>
9. butadiene + ethylene $\leftrightarrow$ cyclohexene	Parent Diels-Alder reaction; Baker et al. <sup>10</sup>
10. s-tetrazine $\leftrightarrow$ 2HCN + N <sub>2</sub>	Baker et al. <sup>10</sup> ; Scheiner et al. <sup>18</sup>
11. trans-butadiene $\leftrightarrow$ cis-butadiene	Baker et al. <sup>10</sup>
12. $\text{CH}_3\text{CH}_3 \leftrightarrow \text{CH}_2\text{CH}_2 + \text{H}_2$	Wolfe and Kim <sup>19</sup>
13. $\text{CH}_3\text{CH}_2\text{F} \leftrightarrow \text{CH}_2\text{CH}_2 + \text{HF}$	Wolfe and Kim <sup>19</sup>
14. vinyl alcohol $\leftrightarrow$ acetaldehyde	Keto-enol tautomerism; Baker et al. <sup>10</sup>
15. $\text{HCOCl} \leftrightarrow \text{HCl} + \text{CO}$	Jasien <sup>20</sup>
16. $\text{H}_2\text{O} + \text{PO}_3^- \leftrightarrow \text{H}_2\text{PO}_4^-$	Ma et al. <sup>21</sup>
17. $\text{CH}_2\text{CHCH}_2\text{-O-CHCH}_2 \leftrightarrow \text{CH}_2\text{CHCH}_2\text{CH}_2\text{CHO}$	Claisen rearrangement; starting geometry from Peng and Schlegel <sup>22</sup>
18. $\text{SiH}_2 + \text{CH}_3\text{CH}_3 \leftrightarrow \text{SiH}_3\text{CH}_2\text{CH}_3$	Silylene insertion; Bach et al. <sup>23</sup>
19. $\text{HNCCS} \leftrightarrow \text{HNC} + \text{CS}$	Flammang et al. <sup>24</sup>
20. $\text{HCONH}_3^+ \leftrightarrow \text{NH}_4^+ + \text{CO}$	Lin et al. <sup>25</sup>
21. rotational TS in acrolein	
22. $\text{HCONHOH} \leftrightarrow \text{HCOHNHO}$	Ventura et al. <sup>26</sup>
23. $\text{HNC} + \text{H}_2 \leftrightarrow \text{H}_2\text{CNH}$	Part of methylenimine PES; Andzelm et al. <sup>27</sup>
24. $\text{H}_2\text{CNH} \leftrightarrow \text{HCNH}_2$	Part of methylenimine PES; Andzelm et al. <sup>27</sup>
25. $\text{HCNH}_2 \leftrightarrow \text{HCN} + \text{H}_2$	Part of methylenimine PES; Andzelm et al. <sup>27</sup>

essential problem here—as already mentioned in the Introduction—is that a perfectly good set of natural internals generated at the starting geometry can easily become unsuitable and badly behaved as the geometry distorts away from standard structures. Of the transition states studied here, system 16 failed to generate a suitable set of internals to begin with, and both systems 6 and 24 failed during the iterative back-transformation to Cartesian coordinates.

Note that the very definition of the Z-matrix—in terms of simple *single* internal variables—eliminates 1 as a problem, and 3 is also avoided, since Cartesians can be generated directly from a given Z-matrix without an iterative procedure; however, 2 can often occur if some thought is not given to Z-matrix construction (e.g., a bond angle going above 180° causing the optimization to abort).

Although situations 1–3 can occur during any optimization in natural internal coordinates and will—for the purposes of this work—cause the optimization to fail, the default in the OPTIMIZE

package is to switch from internal to Cartesian coordinates in such cases and continue the optimization in Cartesians. Thus in real production work, OPTIMIZE will usually find a stationary point irrespective of any problems with the coordinate system.

Looking now at the optimizations in Cartesian coordinates, we see that in no case did any Cartesian optimization converge in fewer cycles than the corresponding Z-matrix optimization, and typically there is a slight increase in the number of cycles required to achieve convergence. In several cases (9, 10, 11, 15, 18, and 19) the Cartesian optimization took three or more cycles *more* than the Z-matrix optimization, with systems 10 (the dissociation of s-tetrazine) and 11 (rotation in butadiene) taking eight and seven more cycles, respectively.

Why should the Cartesian optimizations take more cycles to converge than the internal coordinate optimizations (more than double the number of cycles for systems 10 and 11, the two worst cases)? One possible reason could be the tendency

TABLE II.

Number of Optimization Cycles to Reach Convergence for the Systems Shown in Table I Using Z-Matrix, Natural Internal, and Cartesian Coordinates with (1) Exact Hessian Calculated at Each Cycle; (2) Powell Update; (3) Murtagh-Sargent Update; and (4) Hybrid Powell-MS Update (see Text for More Details).

System	Exact Hessian			Powell Update			MS Update			Powell-MS Update		
	Z-Mat.	Nat. Int.	Cart.	Z-Mat.	Nat. Int.	Cart.	Z-Mat.	Nat. Int.	Cart.	Z-Mat.	Nat. Int.	Cart.
1. C <sub>s</sub>	6	6	7	9	9	10	13	13	15	9	9	10
2. C <sub>s</sub>	5	5	6	8	7	9	6	6	9	8	7	9
3. C <sub>s</sub>	7	7	7	17	16	13	11	12	—	13	16	12
4. C <sub>s</sub>	5	4	5	12	7	7	7	6	7	11	6	7
5. C <sub>1</sub>	8	8	9	12	13	21	—	17	—	11	13	21
6. C <sub>1</sub>	5	—	5	8	43	8	9	—	10	7	44	8
7. C <sub>1</sub>	6	6	7	9	19	24	10	13	—	9	15	20
8. C <sub>1</sub>	5	5	6	31	—	18	12	11	—	26	—	17
9. C <sub>s</sub>	6	7	10	13	16	24	—	—	—	13	16	25
10. C <sub>2v</sub>	6	6	14	17	10	19	9	—	45	14	10	19
11. C <sub>2</sub>	7	6	14	8	8	31	8	8	—	8	8	29
12. C <sub>s</sub>	5	5	6	12	10	9	—	—	10	12	11	9
13. C <sub>s</sub>	6	9	8	12	12	11	—	—	12	11	11	11
14. C <sub>1</sub>	8	8	9	14	13	18	20	14	—	13	13	16
15. C <sub>s</sub>	7	10	10	13	28	17	—	—	—	12	20	17
16. C <sub>1</sub>	7	—	8	24	—	23	—	—	—	23	—	19
17. C <sub>1</sub>	5	5	7	9	7	25	8	14	—	8	7	16
18. C <sub>1</sub>	6	5	9	7	10	21	—	8	—	7	11	21
19. C <sub>s</sub>	6	6	10	10	—	34	12	—	—	10	—	33
20. C <sub>s</sub>	6	6	7	10	10	14	—	14	—	10	10	14
21. C <sub>1</sub>	4	4	4	4	4	5	5	5	6	4	4	5
22. C <sub>s</sub>	4	4	5	5	5	6	6	5	7	5	5	6
23. C <sub>1</sub>	4	4	5	8	8	8	8	8	9	8	8	8
24. C <sub>1</sub>	8	—	8	14	—	16	—	—	20	14	—	18
25. C <sub>1</sub>	5	5	5	9	9	10	9	11	13	9	9	10

The last three systems (23–25; see Table I) actually have C<sub>s</sub> symmetry although the starting geometries were in all cases C<sub>1</sub>. A dash indicates failure to converge within 50 cycles (the maximum allowed); optimizations in natural internal coordinates usually failed due to problems with the coordinate set (see text for more details).

for step sizes in internal coordinate space to be much larger when converted into Cartesian space (this has already been commented on in ref. 4 for natural internals, and the same holds for Z-matrix coordinates). Thus the internal coordinate optimizations could simply take larger steps than the corresponding Cartesian optimizations and hence get to their destination in fewer cycles. While this may be a contributory factor for the rotation in butadiene (system 11)—for which, for example, the first four steps in natural internal coordinates, converted into Cartesian displacements, are 0.705, 0.858, 0.985, and 0.670, respectively, compared to only 0.3 au (the maximum allowed default) in the Cartesian optimization—it is definitely not a factor for the tetrazine decomposition (system 10), for which—due to the composite nature of the natural internal set—the first four steps in internal coordinates are actually *less* (0.248, 0.246, 0.257, and

0.263) in Cartesian space than for the Cartesian optimization (again the maximum allowed value of 0.3 au).

The main reason for the differences in the convergence rate between Cartesians and internals is simply—as previously discussed by Pulay and co-workers<sup>3</sup>—the generally much reduced coupling between the coordinates in the latter case. In the quadratic region of the PES (i.e., near the transition state), then—since we have an exact Hessian—Cartesian coordinates are as good as any other coordinate set, but farther away from the transition state anharmonic terms will become more important and their effect will be *greater* in Cartesian coordinates due to the increased coupling. It is no coincidence that the two worst cases we have highlighted both have starting Hessians with all positive eigenvalues (see Table III) (i.e., nominally closer to minima than to transition

**TABLE III.**  
**Number of Negative Eigenvalues in the Original**  
**(Exact) Starting Hessian for the Systems Shown in**  
**Table I.**

System	Number of Negative Eigenvalues in Starting Hessian Matrix		
	Z-Matrix	Nat. Int.	Cartesians
8.	2	2	2
10.	0	0	0
11.	0	0	0
14.	1	1	2
15.	1	1	0
16.	2	—	3
18.	1	1	2
23.	2	2	1
24.	1	1	2
25.	1	1	2

If no values are given for a particular reaction, then the starting Hessian had the correct local curvature (1 negative Hessian eigenvalue).

states). Thus, for the Cartesian optimizations, we are simply taking poorer quality steps on the PES than in internal space and hence, not surprisingly, we have to take more of them to locate the desired stationary point.

Turning now to the Z-matrix optimizations with the Powell update, we see—not unexpectedly—a significant increase in the number of cycles required to reach convergence, reflecting the approximate nature of the Hessian. The increase is typically 50–100%, but in a few cases it is considerably more than this; the worst examples are the 1,2-migration in the  $\beta$ -(formyloxy) ethyl radical (system 8, increasing from five cycles with an exact Hessian to 31 with the update) and the addition of water to the phosphate anion (system 16; increasing from seven to 24 cycles) (i.e., by factors of more than 5 and 3, respectively). Both these systems had starting Hessians with two negative eigenvalues, and examining the Hessian eigenvalue structure at each optimization cycle shows that this never really stabilized to having the desired one negative eigenvalue until very late in the optimization. This was particularly marked for system 8, which oscillated continuously between having one and two negative Hessian eigenvalues until cycle 26 (on 16 cycles out of the first 25 there were two negative eigenvalues in the Hessian matrix). Examination of the starting Hessian for this system revealed that, for the particular Z-matrix used (see the Appendix), there was major coupling

between the various internal coordinates, with several large off-diagonal Hessian matrix elements often of greater magnitude than the diagonal element in the same column. Additionally, the lowest positive Hessian eigenvalue (when it was positive) was very small and hence did not require too much error in the update to change sign.

We can make a fairly general observation that an updated (as opposed to an exact) Hessian is likely to be much less efficacious when (1) the coordinate set is highly coupled (several large off-diagonal Hessian matrix elements); and (2) there are one or more low energy (floppy) modes (Hessian eigenvalues with small magnitude which can easily change sign during the update). The  $\beta$ -(formyloxy) ethyl radical is a fairly extreme example (it has *both* of these characteristics).

Since Cartesian coordinates are usually more coupled than internals, we would expect Cartesian optimizations using updated Hessians to show an even worse performance vis à vis an exact Hessian than optimizations in internal coordinates, and this is generally borne out by the results in Table II. Compared to the exact Hessian results, although there are many Cartesian optimizations using the Powell update that show an increase in the number of cycles to reach convergence by 50–100%, there are also several that show a larger increase than this, and there are *more* of these than for the Z-matrix optimizations. Of particular note are systems 7, 8, 11, 16, 17, and 19. All of these systems show exactly the same symptoms (although not as marked) as the Z-matrix optimization of  $\beta$ -(formyloxy) ethyl—namely, a change in the Hessian eigenvalue structure (from one to two negative eigenvalues) several times during the course of the optimization with a consequent reduction in the rate of convergence due to the poor steps taken using a Hessian which (often wrongly) had the wrong number of negative eigenvalues.

Comparing the Powell-update Z-matrix and Cartesian optimizations with each other, we see that although there are several systems for which the two coordinate sets show a similar performance, in general the Z-matrix optimizations are significantly better, and in some cases dramatically so. There are five systems for which the Cartesian optimization takes more than twice as many cycles to converge as the corresponding Z-matrix optimization (systems 7, 11, 17, 18, and 19).

Having said that, however, there are three systems for which the Z-matrix optimization takes four or more cycles *more* to converge than the equivalent Cartesian optimization. One of these is

the  $\beta$ -(formyloxy) ethyl radical, already discussed (in which the Cartesian optimization performs a lot better); the other two are the decomposition of formaldehyde (system 3) and the rearrangement of the methoxy radical (system 4). For these two systems, optimizations in both sets of coordinates (Z-matrix and Cartesian) have starting Hessians with the required one negative eigenvalue. The Cartesian optimizations converge smoothly with no change in the Hessian eigenvalue structure. The Z-matrix optimizations, on the other hand, show smooth convergence initially, but midway through the optimization there is a bad Hessian update which changes the eigenvalue structure (from one to zero negative eigenvalues on cycle 6 for the methoxy radical, and from one to two negative eigenvalues on cycle 10 for formaldehyde). The optimization then takes three or four cycles to recover from the bad step taken with the wrong signature Hessian, and it is this one bad update that is responsible for the poor performance of the Z-matrix optimization compared to the corresponding optimization in Cartesian coordinates.

The natural internal coordinate optimizations with the Powell update generally show a similar performance to the corresponding Z-matrix optimizations, although there are some systems that perform better (e.g., 4 and 10) and some that are significantly worse [7, 15, and especially 6—this latter system failed to converge with an exact Hessian calculated at each cycle; it did manage to converge with the Powell update albeit in an enormous number of cycles (43 as compared to 8 in both Z-matrix and Cartesian coordinates) showing that the natural internal coordinates generated in this example were very poor]. Four systems failed to converge: 16 and 24, which both failed even with an exact Hessian, and 8 and 19.

This last system—the dissociation of HNCCS—is instructive as it illustrates what can go wrong with an initially perfectly reasonable set of natural internal coordinates as the molecular geometry changes. A diagram of this system and the starting Z-matrix are given in the Appendix. The set of natural internals generated for HNCCS are particularly simple, being the four obvious interatomic distances appropriate to the given connectivity—note that the C $\cdots$ C “bond” was added to the formal connectivity list in order to generate a full set of coordinates, as discussed in the Introduction—and the individual HNC, NCC, and CCS bond angles (i.e., probably precisely the internal coordinates one would use if one sat down and constructed the first Z-matrix that came to mind).

However, it doesn't take too much chemical intuition to realize that as the system dissociates and the CS fragment leaves, the HNC angle—which has an initial value of  $146^\circ$ —is likely to head toward  $180^\circ$  since the HNC molecule is linear. Bond angles very close to  $180^\circ$  are bad news for geometric conversion algorithms, and what actually happens in this case with the updated Hessian is that a step is taken during the optimization that takes the HNC angle—in the sense shown in the diagram in the Appendix—*above*  $180^\circ$ , causing the back conversion to Cartesian coordinates to fail. Consequently, the natural internal coordinate optimization aborts at the end of cycle 3. When constructing the initial Z-matrix, this possibility is allowed for by introducing a dummy atom to define the HNC bond angle, and the Z-matrix optimization converges smoothly.

Looking at the optimizations using the Murtagh-Sargent update alone (Table II), we can quickly dismiss this update as being unsuitable for general use during transition state searches; there are simply too many cases which fail to converge (13 out of 25 Cartesian optimizations failed to converge within the maximum allowed 50 cycles; more than half of the systems studied). These failures are due entirely to the poor-quality Hessian update. Interestingly, for some of the Z-matrix optimizations, the MS update performs better than the Powell update in a few cases (most notably systems 3, 4, 10, and the pathological system 8, which takes only 12 cycles, down from 31), but the many failures overshadow the improved performance in these few cases (nine of the Z-matrix optimizations fail with the MS update).

Comparing now the results using the combined Powell-MS update proposed by Bofill<sup>11</sup> with the Powell update alone, there is a clear, albeit not especially dramatic, improvement. For the Z-matrix optimizations, none of the systems studied took more cycles to converge with the former update than with the latter, and 11 of them took less. The reduction is typically only one or two cycles, but for three systems (3, 8, and 10) it was three cycles or more. With the Cartesian optimizations, although there were two systems (9 and 24) that took more cycles to converge with the combined update (one and two cycles more, respectively), there were eight that took less, including reductions by four cycles (systems 7 and 16) and nine cycles (system 17). There were also some reductions for the natural internal coordinate optimizations, most notably for the HCOCl decomposition (system 15, reduced from 28 to 20 cycles).



Overall, the hybrid Powell-MS update performs better than the Powell update alone and has consequently been adopted as the default for transition state searches with OPTIMIZE. However, it is clear that better updating schemes are urgently needed for transition state optimizations, especially updates that can preserve the correct Hessian eigenvalue structure once it is found. Some authors recommend a step-reduction scheme<sup>28</sup> in conjunction with standard Hessian updates (see, e.g., refs. 7 and 11); we have not found this to be a particularly advantageous strategy with the EF algorithm. For many years Schlegel has used an updating scheme in his optimization algorithms which uses data from several previous geometries, not just the last one, to improve the Hessian matrix<sup>29</sup>; in common with the more traditional updates, though, this is not guaranteed to preserve the Hessian eigenvalue structure.

Before concluding, we present in Table IV a comparison between the performance of the EF algorithm, as implemented in the OPTIMIZE package,<sup>8</sup> and the default algorithm in GAUSSIAN 90<sup>30</sup> for all of the systems studied in this work. Also given are comparisons with the work of Bofill<sup>11</sup> for the four reactions common to both studies (although only two of these are really appropriate). The GAUSSIAN optimizations used the 3-21G basis and the Z-matrices given in the Appendix, and an exact Hessian was calculated on the first cycle; hence the results are directly comparable with this work.

As can be seen, the EF algorithm with the (now) default Powell-MS update performs very well and is clearly superior to the standard TS algorithm in GAUSSIAN 90. The pathological  $\beta$ -(formyloxy) ethyl radical (system 8) took the same number of cycles to converge with GAUSSIAN 90 as in this work, and many of the other systems took significantly more; two systems failed to converge (surprisingly, one of them was the seemingly innocuous methoxy radical rearrangement, which converged in 11 cycles with the EF algorithm).

Of the two systems that are directly comparable with Bofill's work,<sup>11</sup> one of them took less cycles to converge than in his case (system 5) and the other more (system 8). For the former system—ring opening of the cyclopropyl radical—Bofill claims that the EF algorithm implemented in the GAMESS program<sup>13</sup> took 36 cycles to converge (compared to only 11 in this work) from the same starting geometry and with a Hessian calculated in full on the first cycle. Something seems suspicious here.

The preceding comparisons, along with the ex-

**TABLE IV.**  
Comparison of the EF Algorithm in OPTIMIZE with the Default Algorithm in GAUSSIAN 90 and the Work of Bofill.<sup>11</sup>

System	Number of Cycles to Reach Convergence		
	This Work <sup>a</sup>	GAUSSIAN 90 <sup>b</sup>	Bofill <sup>c</sup>
1.	9	11	
2.	8	7	
3.	13	10	
4.	11	—	12
5.	11	18	19
6.	7	11	11
7.	9	13	9
8.	26	26	22
9.	13	14	
10.	14	21	
11.	8	9	
12.	12	17	
13.	11	16	
14.	13	16	
15.	12	13	
16.	23	—	
17.	8	18	
18.	7	10	
19.	10	10	
20.	10	13	
21.	4	4	
22.	5	6	
23.	8	7	
24.	14	27	
25.	9	11	

All optimizations started from the Z-matrices given in the Appendix; an exact Hessian matrix was calculated on the first cycle only.

<sup>a</sup>Using the Powell-MS update; numbers as per Z-matrix column of Table II.

<sup>b</sup>A dash denotes failure to converge in 50 cycles.

<sup>c</sup>Only systems 5 and 8 are directly comparable with Bofill's work; the other systems reported used the same starting geometry but a different Hamiltonian.

cellent performance when exact Hessian data is available (Table II), show that the EF algorithm is extremely efficient for optimizing transition states.

## Conclusions

Although previous work<sup>1,4</sup> has demonstrated that, provided a reliable estimate of the Hessian matrix is available at the (reasonable) starting geometry, minimization in Z-matrix, natural internal, and Cartesian coordinates is of comparable efficiency, for transition state searches a good-quality Z-matrix is generally superior.

That this is the case is due in part to the fact that starting geometries for transition state optimizations are usually much farther from the final converged structure than is typically the case for minimization (for which molecular mechanics force fields can provide both reliable starting geometries and Hessians), and the increased coupling in Cartesian coordinates at such poor starting geometries slows down the convergence. This is true even with exact second derivatives available at each optimization cycle.

This situation is exacerbated when updated (approximate) Hessians are used in Cartesian optimizations as the coupling makes it difficult to maintain the desired Hessian eigenvalue structure (one and only one negative eigenvalue) and, once this is lost, the optimization can take poor or misguided steps on the potential energy surface, severely inhibiting convergence. This can occur even with internal coordinate optimizations, but it is much less likely due to the reduced coupling with a good set of internals. Such effects are particularly marked in systems with one or more floppy modes (modes associated with small Hessian eigenvalues).

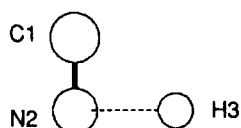
Although natural internal coordinates might be expected to reduce the coupling between the individual internal coordinates even more than with a Z-matrix, the distorted, nonstandard geometries

associated with transition states make it hard to construct and maintain a good set of natural internals (which were designed primarily for minimization). In particular, perfectly adequate natural internal coordinates constructed at the starting geometry could become inappropriate as the geometry distorts during the optimization, hindering convergence or causing the optimization to fail.

A viable strategy for transition state searches might be to describe the atoms involved in the active site (those where most of the geometrical changes are taking place) in terms of individual, Z-matrix-like, internal coordinates, or even Cartesians if this is deemed appropriate, and any side chains or other structures which are not part of the active site in terms of natural internals. Hessian information would then only be needed for the active site atoms; the side chains—described using natural internals—could be successfully optimized without second derivative data. Work along these lines is currently in progress.

## Appendix

Z-matrices with starting parameters, initial energies, and final energies (at convergence) for the test suite of 25 transition states given in Table I.

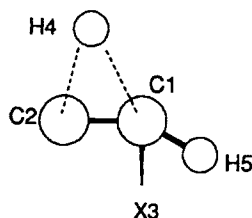


C1					
N2	1	L1			
H3	2	L2	1	A1	

L1	1.14838
L2	1.58536
A1	90.0

1. HCN <-> HNC

$E_{init}$	-92.20273	$E_{final}$	-92.24604
------------	-----------	-------------	-----------

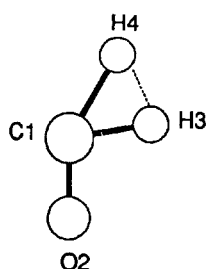


C1							
C2	1	L1					
X3	1	1.0	2	90.0			
H4	1	L2	2	A1	3	180.0	
H5	1	L3	3	A2	2	180.0	

L1	1.24054
L2	1.65694
L3	1.06318
A1	60.3568
A2	60.3568

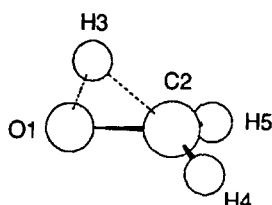
2. HCCH <-> CCH<sub>2</sub>

$E_{init}$	-76.26542	$E_{final}$	-76.29343
------------	-----------	-------------	-----------



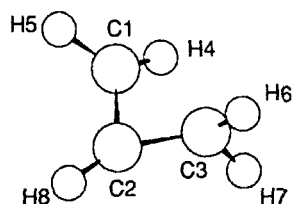
C1							
O2	1	L1					
H3	1	L2	2	A1			
H4	1	L3	2	A2	3	0.0	

L1	1.25
L2	1.3
L3	1.5
A1	100.0
A2	150.0

3.  $\text{H}_2\text{CO} \leftrightarrow \text{H}_2 + \text{CO}$  $E_{\text{init}}$  -112.98005 $E_{\text{final}}$  -113.05003

O1							
C2	1	L1					
H3	2	L2	1	A1			
H4	2	L3	1	A2	3	D1	
H5	2	L3	1	A2	3	-D1	

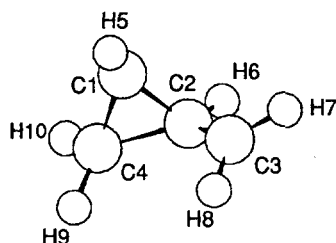
L1	1.423
L2	1.484
L3	1.087
A1	42.7
A2	117.5
D1	106.4

4.  $\text{CH}_3\text{O} \leftrightarrow \text{CH}_2\text{OH}$  $E_{\text{init}}$  -113.71655 $E_{\text{final}}$  -113.69365

C1							
C2	1	L1					
C3	2	L2	1	A1			
H4	1	L3	2	A2	3	D1	
H5	1	L4	2	A3	3	D2	
H6	3	L5	2	A4	1	D3	
H7	3	L6	2	A5	1	D4	
H8	2	L7	3	A6	1	D5	

L1	1.454	A1	80.0
L2	1.454	A2	119.6
L3	1.106	A3	119.6
L4	1.106	A4	119.6
L5	1.106	A5	119.6
L6	1.106	A6	148.5
L7	1.064	D1	40.0
		D2	-160.0
		D3	108.0
		D4	-108.0
		D5	-170.0

5. ring opening cyclopropyl

 $E_{\text{init}}$  -115.67622 $E_{\text{final}}$  -115.72100

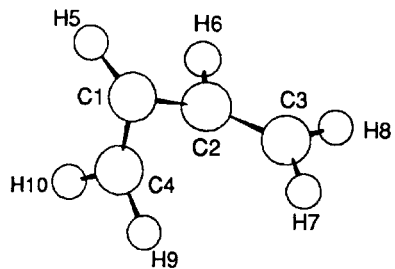
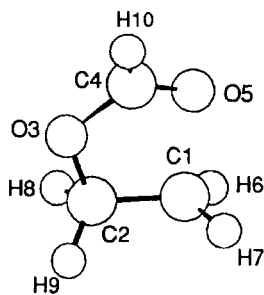
C1							
C2	1	L1					
C3	2	L2	1	A1			
C4	1	L3	2	A2	3	D1	
H5	1	L4	2	A3	3	D2	
H6	2	L5	1	A4	4	D3	
H7	3	L6	2	A5	1	D4	
H8	3	L7	2	A6	1	D5	
H9	4	L8	1	A7	2	D6	
H10	4	L9	1	A8	2	D7	

L1	1.495	A3	136.0
L2	1.418	A4	123.5
L3	1.463	A5	122.4
L4	1.093	A6	124.7
L5	1.111	A7	126.7
L6	1.098	A8	117.9
L7	1.097	D1	-120.4
L8	1.110	D2	4.4
L9	1.106	D3	108.8
A1	92.1	D4	-107.5
A2	62.1	D5	84.2
		D6	109.3
		D7	-106.1

6. bicyclo[1.1.0] butane TS 1

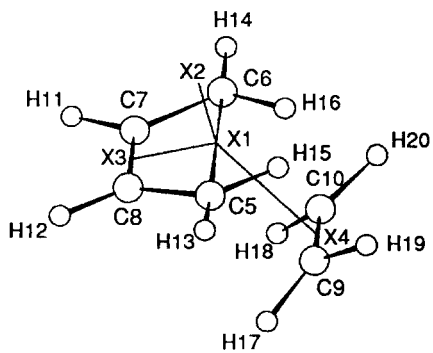
 $E_{\text{init}}$  -153.88777 $E_{\text{final}}$  -153.90494

## LOCATION OF TRANSITION STATES

[illegible]7. bicyclo[1.1.0] butane TS 2  $E_{init}$  -153.87578  $E_{final}$  -153.89754[illegible]

8.  $\beta$ -(formyloxy) ethyl

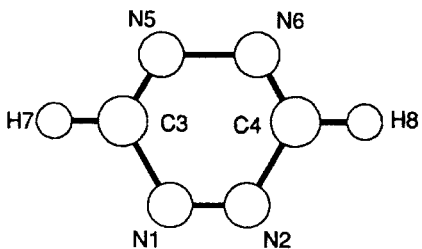
**E<sub>init</sub> -264.63426      E<sub>final</sub> -264.64757**



X1						L1	1.2
X2	1	1.0				L2	2.0
X3	1	L1	2	90.0		L3	1.4
X4	1	L2	2	A1	3	L4	0.7
C5	1	L3	3	90.0	2	L5	0.7
C6	1	L3	3	90.0	2	L6	1.0
C7	3	L4	1	90.0	2	L7	1.0
C8	3	L4	1	90.0	2	L8	1.0
C9	4	L5	1	90.0	2	L9	1.0
C10	4	L5	1	90.0	2	L10	1.0
H11	7	L6	6	A2	1	A1	150.
H12	8	L6	5	A2	1	A2	120.
H13	5	L7	8	A3	3	A3	118.
H14	6	L7	7	A3	3	A4	118.
H15	5	L8	8	A4	3	A5	118.
H16	6	L8	7	A4	3	A6	118.
H17	9	L9	4	A5	1	D1	175.
H18	10	L9	4	A5	1	D2	175.
H19	9	L10	4	A6	1	D3	-6.
H20	10	L10	4	A6	1	D4	95.
						D5	-96.

9. parent Diels-Alder

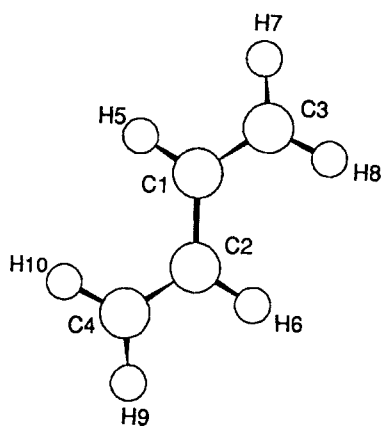
**E<sub>init</sub> -231.48964      E<sub>final</sub> -231.60321**



N1							L1	1.20
N2	1	L1					L2	1.50
C3	1	L2	2	A1			L3	1.20
C4	2	L2	1	A1	3	0.0	L4	1.08
N5	3	L3	1	A2	2	0.0	A1	120.0
N6	4	L3	2	A2	1	0.0	A2	120.0
H7	3	L4	5	A3	6	180.0	A3	120.0
H8	4	L4	6	A3	5	180.0		

10. s-tetrazine  $\leftrightarrow$  2HCN + N<sub>2</sub>

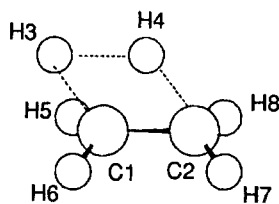
**E<sub>init</sub>   -292.84863      E<sub>final</sub>   -292.81026**



C1						
C2	1	L1				
C3	1	L2	2	A1		
C4	2	L2	1	A1	3	D1
H5	1	L3	2	A2	4	D2
H6	2	L3	1	A2	3	D2
H7	3	L4	1	A3	2	D3
H8	3	L5	1	A4	2	D4
H9	4	L4	2	A3	1	D3
H10	4	L5	2	A4	1	D4

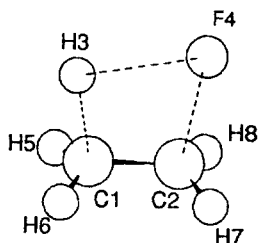
L1	1.467
L2	1.320
L3	1.08
L4	1.081
L5	1.082
A1	124.0
A2	121.0
A3	119.0
A4	121.0
D1	160.0
D2	-20.0
D3	180.0
D4	0.0

11. rotational TS in butadiene

 $E_{\text{init}}$  -154.05460 $E_{\text{final}}$  -154.05046

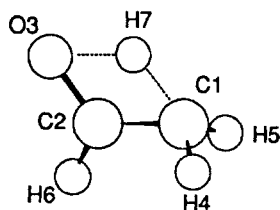
C1						
C2	1	L1				
H3	1	L2	2	A1		
H4	2	L3	1	A2	3	0.0
H5	1	L4	2	A3	3	D1
H6	1	L4	2	A3	3	-D1
H7	2	L5	1	A4	4	D2
H8	2	L5	1	A4	4	-D2

L1	1.43
L2	1.50
L3	1.50
L4	1.09
L5	1.09
A1	120.0
A2	60.0
A3	115.0
A4	115.0
D1	104.0
D2	104.0

12.  $\text{CH}_3\text{CH}_3 \leftrightarrow \text{CH}_2\text{CH}_2 + \text{H}_2$  $E_{\text{init}}$  -78.55086 $E_{\text{final}}$  -78.54323

C1						
C2	1	L1				
H3	1	L2	2	A1		
F4	2	L3	1	A2	3	0.0
H5	1	L4	2	A3	4	D1
H6	1	L4	2	A3	4	-D1
H7	2	L5	1	A4	4	D2
H8	2	L5	1	A4	4	-D2

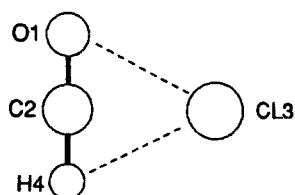
L1	1.43
L2	1.50
L3	1.90
L4	1.08
L5	1.08
A1	100.0
A2	100.0
A3	115.0
A4	115.0
D1	105.0
D2	105.0

13.  $\text{CH}_3\text{CH}_2\text{F} \leftrightarrow \text{CH}_2\text{CH}_2 + \text{HF}$  $E_{\text{init}}$  -176.96525 $E_{\text{final}}$  -176.98453

C1						
C2	1	L1				
O3	2	L2	1	A1		
H4	1	L3	2	A2	3	D1
H5	1	L4	2	A3	3	D2
H6	2	L5	1	A4	3	D3
H7	3	L6	2	A5	1	D4

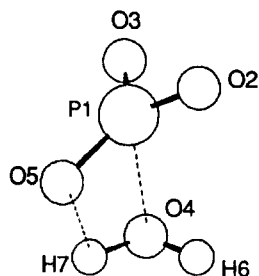
L1	1.43	A1	120.0
L2	1.30	A2	110.0
L3	1.09	A3	110.0
L4	1.09	A4	120.0
L5	1.09	A5	60.0
L6	1.35	D1	115.0
		D2	-120.0
		D3	175.0
		D4	5.0

14.  $\text{CH}_2\text{CHOH} \leftrightarrow \text{CH}_3\text{CHO}$  $E_{\text{init}}$  -151.87756 $E_{\text{final}}$  -151.91310



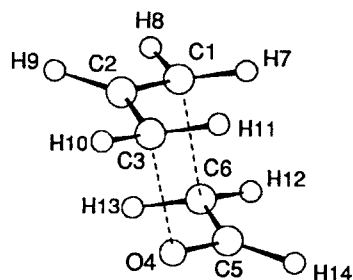
O1						
C2	1	L1				
CL3	2	L2	1	A1		
H4	2	L3	3	A2	1	180.0

L1	1.17
L2	2.335
L3	1.127
A1	90.0
A2	90.0

15. HCOCl <=> HCl + CO $E_{init}$  -569.87865 $E_{final}$  -569.89752

P1						
O2	1	L1				
O3	1	L2	2	A1		
O4	1	L3	2	A2	3	D1
O5	1	L4	2	A3	3	D2
H6	4	L5	1	A4	2	D3
H7	5	L6	1	A5	2	D4

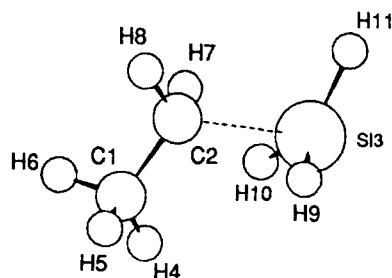
L1	1.46	A1	109.47
L2	1.46	A2	109.47
L3	1.98	A3	125.02
L4	1.54	A4	109.5
L5	0.95	A5	109.5
L6	1.27	D1	120.0
		D2	-172.35
		D3	0.74
		D4	-84.48

16. H2O + PO3- <=> H2PO4- $E_{init}$  -637.78814 $E_{final}$  -637.92388

C1						
C2	1	L1				
C3	2	L2	1	A2		
O4	3	L3	2	A3	1	D3
C5	4	L4	3	A4	2	D4
C6	5	L5	4	A5	3	D5
H7	1	R1	2	AH1	3	DH1
H8	1	R2	2	AH2	3	DH2
H9	2	R3	1	AH3	3	DH3
H10	3	R4	2	AH4	1	DH4
H11	3	R5	2	AH5	1	DH5
H12	6	R6	5	AH6	4	DH6
H13	6	R7	5	AH7	4	DH7
H14	5	R8	6	AH8	4	DH8

L1	1.420	AH1	115.0
L2	1.405	AH2	115.0
L3	2.008	AH3	120.0
L4	1.310	AH4	115.0
L5	1.410	AH5	115.0
R1	1.09	AH6	115.0
R2	1.09	AH7	115.0
R3	1.09	AH8	120.0
R4	1.09	D3	-66.8
R5	1.09	D4	56.6
R6	1.09	D5	-67.8
R7	1.09	DH1	-30.0
R8	1.09	DH2	180.0
A2	120.0	DH3	180.0
A3	101.1	DH4	180.0
A4	103.5	DH5	30.0
A5	120.0	DH6	180.0
		DH7	-30.0
		DH8	180.0

17. Claisen rearrangement

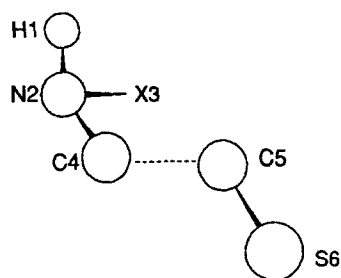
 $E_{init}$  -267.21899 $E_{final}$  -267.23859

C1						
C2	1	L1				
Si3	2	L2	1	A1		
H4	1	L3	2	A2	3	D1
H5	1	L4	2	A3	3	D2
H6	1	L5	2	A4	3	D3
H7	2	L6	1	A5	3	D4
H8	2	L7	1	A6	3	D5
H9	3	L8	2	A7	1	D6
H10	3	L9	2	A8	1	D7
H11	3	L10	2	A9	1	D8

L1	1.52	A4	108.63
L2	2.30	A5	108.12
L3	1.10	A6	108.93
L4	1.09	A7	108.93
L5	1.11	A8	41.00
L6	1.09	A9	109.12
L7	1.10	D1	-65.13
L8	1.48	D2	62.27
L9	1.50	D3	178.92
L10	1.48	D4	121.91
A1	119.26	D5	-122.55
A2	114.17	D6	-55.52
A3	115.06	D7	65.18
		D8	-174.11

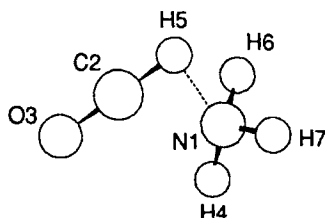
18. silylene insertion

 $E_{init}$  -367.19458 $E_{final}$  -367.20778



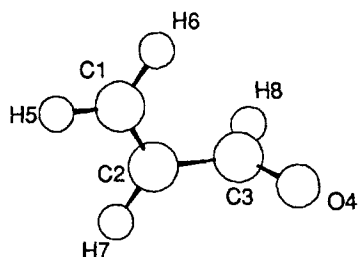
H1						
N2	1	L1				
X3	2	L2	1	90.0		
C4	2	L2	3	A1	1	180.0
C5	4	L3	2	A2	3	0.0
S6	5	L4	4	A3	2	180.0

L1	1.01
L2	1.2
L3	1.86
L4	1.57
A1	56.0
A2	128.5
A3	124.9

19. HNCCS  $\leftrightarrow$  HNC + CS $E_{\text{init}}$  -525.42284  $E_{\text{final}}$  -525.43040

N1						
C2	1	L1				
O3	2	L2	1	A1		
H4	1	L3	2	A2	3	0.0
H5	2	L4	1	A3	4	180.0
H6	1	L5	2	A4	3	D1
H7	1	L5	2	A4	3	-D1

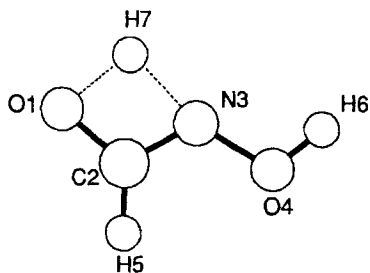
L1	2.0
L2	1.13
L3	1.03
L4	1.08
L5	1.03
A1	120.0
A2	109.5
A3	60.0
A4	109.5
D1	120.0

20. HCONH<sub>3</sub><sup>+</sup>  $\leftrightarrow$  NH<sub>4</sub><sup>+</sup> + CO $E_{\text{init}}$  -168.23208  $E_{\text{final}}$  -168.24752

C1						
C2	1	L1				
C3	2	L2	1	A1		
O4	3	L3	2	A2	1	D1
H5	1	L4	2	A3	3	D2
H6	1	L5	2	A4	3	D3
H7	2	L6	1	A5	3	D4
H8	3	L7	2	A6	4	D5

L1	1.34	A3	120.0
L2	1.45	A4	120.0
L3	1.22	A5	120.0
L4	1.08	A6	120.0
L5	1.08	D1	90.0
L6	1.08	D2	180.0
L7	1.08	D3	0.0
A1	120.0	D4	180.0
A2	120.0	D5	180.0

21. rotational TS in acrolein

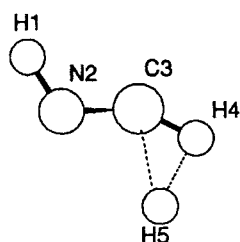
 $E_{\text{init}}$  -189.67124  $E_{\text{final}}$  -189.67574

O1						
C2	1	L1				
N3	2	L2	1	A1		
O4	3	L3	2	A2	1	180.0
H5	2	L4	3	A3	4	0.0
H6	4	L5	3	A4	2	180.0
H7	3	L6	2	A5	1	0.0

L1	1.3	A1	110.0
L2	1.3	A2	120.0
L3	1.4	A3	120.0
L4	1.1	A4	109.6
L5	1.0	A5	75.0
L6	1.5		

22. HCONHOH  $\leftrightarrow$  HCOHNHO $E_{\text{init}}$  -242.24912  $E_{\text{final}}$  -242.25529

# LOCATION OF TRANSITION STATES



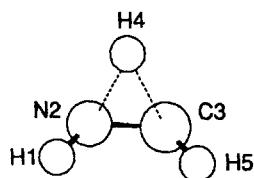
H1						
N2	1	L1				
C3	2	L2	1	A1		
H4	3	L3	2	A2	1	D1
H5	4	L4	3	A3	2	D2

L1	1.0
L2	1.2
L3	1.0
L4	1.2
A1	120.0
A2	150.0
A3	90.0
D1	170.0
D2	10.0

23. HNC + H2 <=> H2CNH

$E_{init}$  -93.30097

$E_{final}$  -93.31114



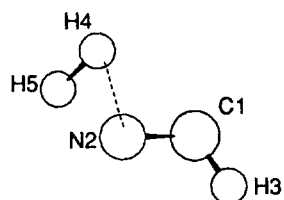
H1						
N2	1	L1				
C3	2	L2	1	A1		
H4	3	L3	2	A2	1	D1
H5	3	L4	2	A3	1	D2

L1	1.0
L2	1.2
L3	1.3
L4	1.0
A1	120.0
A2	60.0
A3	120.0
D1	-120.0
D2	0.0

24. H2CNH <=> HCNH2

$E_{init}$  -93.29435

$E_{final}$  -93.33296



C1						
N2	1	L1				
H3	1	L2	2	A1		
H4	2	L3	1	A2	3	D1
H5	2	L4	1	A3	3	D2

L1	1.35
L2	1.0
L3	1.4
L4	1.4
A1	105.0
A2	105.0
A3	110.0
D1	150.0
D2	-160.0

25. HCNH2 <=> HCN + H2

$E_{init}$  -93.25640

$E_{final}$  -93.28172



---

## References

1. J. Baker and W. J. Hehre, *J. Comput. Chem.*, **12**, 606 (1991).
2. P. Pulay, G. Fogarasi, F. Pang, and J. E. Boggs, *J. Am. Chem. Soc.*, **101**, 2550 (1979).
3. G. Fogarasi, X. Zhou, P. W. Taylor, and P. Pulay, *J. Am. Chem. Soc.*, **114**, 8191 (1992).
4. J. Baker, *J. Comput. Chem.*, **14**, 1085 (1993).
5. J. Baker, *J. Comput. Chem.*, **7**, 385 (1986).
6. C. J. Cerjan and W. H. Miller, *J. Chem. Phys.*, **75**, 2800 (1981).
7. A. Banerjee, N. Adams, J. Simons, and R. Shepard, *J. Phys. Chem.*, **89**, 52 (1985).
8. J. Baker, OPTIMIZE, version 1.0 beta, Biosym Technologies, San Diego, CA 1993.
9. R. Ahlrichs, M. Bär, M. Ehrig, M. Häser, H. Horn, and C. Kölmel, TURBOMOLE, version 2.2 beta, Biosym Technologies, San Diego, CA, 1993.
10. J. Baker, M. Muir, and J. Andzelm, *J. Chem. Phys.*, **102**, 2063 (1995).
11. J. M. Bofill, *J. Comput. Chem.*, **15**, 1 (1994).
12. J. J. P. Stewart, MOPAC, version 5.0, program 455, Quantum Chemistry Program Exchange, Indiana University, Bloomington, IN.
13. M. Dupuis, D. Spangler, and J. J. Wendoloski, GAMESS, Nat. Resour. Comput. Chem. Software Cat., program QG01, 1980; extended by M. W. Schmidt and S. T. Elbert, 1992.
14. M. J. D. Powell, *Math. Prog.*, **1**, 26 (1971).
15. B. A. Murtagh and R. W. H. Sargent, *Comput. J.*, **13**, 185 (1970).
16. E. B. Wilson, J. C. Decius, and P. C. Cross, *Molecular Vibrations*, McGraw-Hill, New York, 1955.
17. P. Pulay, In *Applications of Electronic Structure Theory*, H. F. Schaefer, Ed., Plenum, New York, 1977, p. 153.
18. A. C. Scheiner, G. E. Scuseria, and H. F. Schaefer III, *J. Am. Chem. Soc.*, **108**, 8160 (1986).
19. S. Wolfe and C-K. Kim, *Israel J. Chem.*, **33**, 295 (1993).
20. P. G. Jasien, *J. Phys. Chem.*, **98**, 2859 (1994).
21. B. Ma, Y. Xie, M. Shen, P. v. R. Schleyer, and H. F. Schaefer III, *J. Am. Chem. Soc.*, **115**, 11169 (1993).
22. C. Peng and H. B. Schlegel, *Israel J. Chem.*, **33**, 449 (1993).
23. R. D. Bach, M-D. Su, E. Aldabbagh, J. L. Andres, and H. B. Schlegel, *J. Am. Chem. Soc.*, **115**, 10237 (1993).
24. R. Flammang, D. Landu, S. Laurent, M. Barbieux-Flammang, C. O. Kappe, M. W. Wong, and C. Wentrup, *J. Am. Chem. Soc.*, **116**, 2005 (1994).
25. H-Y. Lin, D. P. Ridge, E. Uggerud, and T. Vulpus, *J. Am. Chem. Soc.*, **116**, 2996 (1994).
26. O. N. Ventura, J. B. Rama, L. Turi, and J. J. Dannenberg, *J. Am. Chem. Soc.*, **115**, 5754 (1993).
27. J. Andzelm, J. Baker, A. C. Scheiner, and M. Wrinn, *Int. J. Quant. Chem.*, **56**, 733 (1995).
28. R. Fletcher, *Practical Methods of Optimization: Unconstrained Optimization*, Vol. 1, John Wiley & Sons, New York, 1980.
29. H. B. Schlegel, *J. Comput. Chem.*, **3**, 214 (1982).
30. M. J. Frisch, M. Head-Gordon, G. W. Trucks, J. B. Foresman, H. B. Schlegel, K. Raghavachari, M. A. Robb, J. S. Binkley, C. Gonzalez, D. J. Defrees, D. J. Fox, R. A. Whiteside, R. Seeger, C. F. Melius, J. Baker, R. L. Martin, L. R. Kahn, J. J. P. Stewart, S. Topiol, and J. A. Pople, Gaussian 90, Revision I, Gaussian Inc., Pittsburgh PA, 1990.